From www.bloodjournal.org by guest on July 26, 2016. For personal use only.
Blood First Edition Paper, prepublished online June 6, 2016; DOI 10.1182/blood-2016-01-690743

DEPENDENCE ON GLUTAMINE UPTAKE AND GLUTAMINE ADDICTION CHARACTERIZE MYELOMA CELLS: A NEW ATTRACTIVE TARGET

SHORT TITLE: Glutamine addiction of myeloma cells

Marina Bolzoni[1]#, Martina Chiu[2]#, Fabrizio Accardi[1,3]#, Rosanna Vescovini[1], Irma Airoldi[5], Paola Storti[1,4], Katia Todoerti[6], Luca Agnelli[7], Gabriele Missale[8], Roberta Andreoli[9], Massimiliano G. Bianchi[2,9], Manfredi Allegri[2], Amelia Barilli[2], Francesco Nicolini[10], Albertina Cavalli[8], Federica Costa[1], Valentina Marchica[1,4], Denise Toscani[1], Cristina Mancini[11], Eugenia Martella[11], Valeria Dall'Asta[2], Gaetano Donofrio[12], Franco Aversa[1,3], Ovidio Bussolati[2] and Nicola Giuliani[1,3,4]

[1]Myeloma Unit, Dept. of Clinical and Experimental Medicine, University of Parma, Parma, Italy; [2]Unit of General Pathology, Dept. of Biomedical, Biotechnological and Translational Sciences, University of Parma, Parma, Italy; [3]Hematology and BMT Center, "Azienda Ospedaliero-Universitaria di Parma", Parma, Italy; [4]CoreLab, "Azienda Ospedaliero-Universitaria di Parma", Parma, Italy; [5]"Laboratorio di Oncologia", "Istituto Giannina Gaslini", Genoa, Italy; [6]Lab. of Pre-clinical and Translational Research, IRCCS, Referral Cancer Center of Basilicata, Rionero in Vulture, Italy; [7]Dept. of Oncology and Hemato-oncology, University of Milan, Milan, Italy; [8]Infectious Disease Unit and Hepatology Unit, "Azienda Ospedaliero-Universitaria di Parma", Parma, Italy; [9]Unit of Occupational Medicine, Dept. of Clinical and Experimental Medicine, University of Parma, Parma, Italy; [10]Cardiac Surgery Unit, Dept. of Clinical and Experimental Medicine, University of Parma; [11]"U.O. di Anatomia Patologica, Azienda Ospedaliero-Universitaria di Parma", Parma, Italy and [12] Dept. of Medical-Veterinary Science, University of Parma, Parma, Italy

# These Authors equally contributed to the study.

Scientific category: Lymphoid Neoplasia
Word count: Text: 4000, Abstract: 250
Figures/Tables count: 7
References count: 59

Addresses Correspondence to:
Nicola Giuliani, MD, PhD
Myeloma Unit, Dept. of Clinical and Experimental Medicine
University of Parma
Via Gramsci 14, 43126, Parma, Italy
Tel: +390521033299; Fax: +390521033271
Email: nicola.giuliani@unipr.it

Copyright © 2016 American Society of Hematology

From www.bloodjournal.org by guest on July 26, 2016. For personal use only.

Ovidio Bussolati, MD, PhD
Unit of General Pathology, Dept. of Biomedical, Biotechnological and Translational Sciences
University of Parma
Via Volturno 39, 43125, Parma, Italy
Tel: +390521033783; Fax: +390521033742
Email: ovidio.bussolati@unipr.it

From www.bloodjournal.org by guest on July 26, 2016. For personal use only.

Key points

- Myeloma cells produce ammonium in the presence of glutamine, showing high Glutaminase and low Glutamine Synthetase expression.
- Myeloma cells show high expression of glutamine transporters and inhibition of ASCT2 transporter hinders myeloma growth.

Abstract

The importance of glutamine (Gln) metabolism in multiple myeloma (MM) cells and its potential role as a therapeutic target are still unknown, although it has been reported that human myeloma cell lines (HMCLs) are highly sensitive to Gln depletion. In this study, we found that both HMCLs and primary bone marrow (BM) $CD138^+$ cells produced large amounts of ammonium in the presence of Gln. MM patients have lower BM plasma Gln with higher ammonium and glutamate than patients with indolent monoclonal gammopathies. Interestingly, HMCLs expressed Glutaminase (GLS1) and were sensitive to its inhibition, while exhibited negligible expression of Glutamine Synthetase (GS). High GLS1 and low GS expression were also observed in primary $CD138^+$ cells. Gln-free incubation or treatment with the glutaminolytic enzyme L-Asparaginase depleted the cell contents of Gln, glutamate and the anaplerotic substrate 2-oxoglutarate, inhibiting MM cell growth. Consistent with the dependence of MM cells on extracellular Gln, a gene expression profile analysis, on both proprietary and published datasets, showed an increased expression of the Gln transporters SNAT1, ASCT2, and LAT1 by $CD138^+$ cells across the progression of monoclonal gammopathies. Among these transporters, only ASCT2 inhibition in HMCLs caused a marked decrease in Gln uptake and a significant fall in cell growth. Consistently, stable ASCT2 down-regulation by a lentiviral approach inhibited HMCL growth *in vitro* and in a murine model. In conclusion, MM cells strictly depend upon extracellular Gln and show features of Gln addiction. Therefore, the inhibition of Gln uptake is a new attractive therapeutic strategy for MM.

From www.bloodjournal.org by guest on July 26, 2016. For personal use only.

INTRODUCTION

Multiple Myeloma (MM) is characterized by the accumulation of malignant plasma cells (PCs) into the bone marrow (BM).[1,2] It is a historical notion that the growth of MM cells was limited by depletion of L-glutamine (Gln)[3] and that MM cells may produce an excess of ammonium (NH_4^+).[4,5] Hyperammonemia with or without the related encephalopathy has been reported as a possible rare clinical manifestation in relapsed/refractory MM patients with high mortality rate.[6-12] Recently, multivariate analysis based on ^{1}H-NMR spectroscopy analysis of serum samples has shown that a specific metabolic profile characterized MM patients *versus* healthy controls, including Gln levels significantly lower in the MM group.[13] Overall, these data suggest that Gln is highly metabolized in MM cells. To satisfy metabolic requirements of Gln, mammalian cells rely on Glutamine Synthetase (GS), the enzyme that obtains Gln from glutamate (Glu) and NH_4^+.[14,15] Moreover, a variety of carriers, operate Gln influx, such as the Na^+-dependent transporters SNAT1-2 and ASCT2, and the Na^+-independent transporter LAT1.[16] Gln is a substrate of several enzymes, playing an important role in various processes, such as the synthesis of nucleotides, other amino acids, or glucosamine.[17,18] Moreover, through the activity of Glutaminases (GLS1 and GLS2), which hydrolyze the amide group obtaining NH_4^+ and Glu, Gln may fuel the intracellular pool of the Krebs cycle intermediate and anaplerotic substrate 2-oxoglutarate (2-OG, α-ketoglutarate).[17,18] Some types of human tumor cells exhibit an high requirement for Gln ("glutamine addiction")[15] and use large amounts of the amino acid as an anaplerotic substrate.[19-21] A number of metabolic features have been described in Gln addicted cancer cells, such as high GS expression[22] or high expression and/or activity of Gln transporters, such as ASCT2.[23] In Gln-addicted cancers, GLS1 inhibition, Gln transporter silencing, inhibitors of Gln uptake or Gln-depleting treatments lead to delayed or arrested tumor growth.[24-26] Gln depletion produces a severe metabolic stress and cell death in some types of acute myeloid leukemia (AML)[27,28] and in Gln-addicted lymphoid cells.[29] Moreover, L-Asparaginase (ASNase), the mainstay in the treatment of acute lymphoblastic leukemia (ALL),[30,31] hydrolyzes not only asparagine but also Gln, and Gln depletion is the main biochemical mechanism underlying the growth inhibition by ASNase in asparagine synthetase-

From www.bloodjournal.org by guest on July 26, 2016. For personal use only.

positive ALL cells.[32] Actually, the relationship between NH_4^+ production and Gln-addiction in MM cells, as well as the mechanisms involved therein, are unknown, and were investigated in this study.

PATIENTS, MATERIALS AND METHODS

Patients

A total cohort of 65 patients (30 males and 35 females) with PC disorders were included in the study: 6 patients with monoclonal gammopathy of undetermined significance (MGUS) (median age: 68 years; range: 44-80), 12 with smoldering myeloma (SMM) (median age: 68 years; range: 41-83), and 46 with active MM (median age: 75 years; range: 43-90) including 28 newly diagnosed MM (ND-MM) and 18 relapsed MM (R-MM). The main clinical characteristics of all the patients enrolled in the study are summarized in Table S1. Adverse cytogenetic/fluorescence in situ hybridization (FISH) refers to unfavorable IgH translocations (t(4;14) or t(14;16) or t(14;20)), 17p13 del and/or 1q21 gain.[33,34] A total cohort of 9 controls (patients without monoclonal gammopathy with cardiac disease; median age: 58 years; range: 42-72) underwent cardiac surgery and were included in the study to obtain normal PCs.

The University of Parma institutional review board (Parma, Italy) approved all the study protocols. All of the patients and controls included in the study gave their written informed consent as laid down in the Declaration of Helsinki.

BM aspirates (5+5 mL, treated with EDTA to prevent clotting) were obtained from the iliac crest of MM, SMM and MGUS patients or from the sternum of controls. BM plasma was collected from 17 MM patients (9 ND-MM and 8 R-MM; ISS: 18% stage I, 35% II and 47% III; adverse FISH: 64%) and 13 patients with indolent monoclonal gammopathies (MGUS and/or SMM) after centrifugation, and stored at -20°C until the analysis. Peripheral blood (PB) was obtained from 21 of 46 MM patients (13 ND-MM and 8 R-MM; ISS: 23% I, 28% II and 48% III; adverse FISH: 29%).

From www.bloodjournal.org by guest on July 26, 2016. For personal use only.

BM cell purification

Both $CD138^+$ PCs and $CD138^-$ cell fractions were isolated from BM mononuclear cells (MNCs) by an immunomagnetic method with anti-CD138 mAb conjugated with microbeads (Miltenyi Biotech; Bergisch-Gladbach, Germany) from 38 patients (2 MGUS, 7 SMM, 29 MM, including 17 ND-MM and 12 R-MM) and 4 out of 9 controls as previously described.[35] FISH analysis was performed on $CD138^+$ PCs as previously described.[36]

Cell lines, reagents and cell treatments

Cell lines and reagents were described in Supplementary Materials and Methods.

Treatment under Gln-free conditions was performed incubating cells in Gln-free RPMI-1640 medium supplemented with 10% FBS dialyzed against a 40x volume of 0.154 M NaCl.

Treatment with *E. chrysanthemi* ASNase (L-asparagine amido hydrolase, E.C. 3.5.1.1, (Jazz Pharmaceuticals Ltd, Oxford, UK)) or with the *E. coli* ASNase (Sigma-Aldrich, Milan, Italy) at concentrations ranging from 0.0001 to 1 U/mL was performed for 48h in RPMI-1640 medium plus 10% FBS and Gln at 4 mM. Bortezomib (Janssen-Cilag, Milan, Italy) dose response (concentration range: 1.77-10 nM) was performed in standard growth medium in the presence or in the absence of 0.1 U/mL of *E. chrysanthemi* ASNase for 48 h. Moreover HMCLs were treated with bortezomib (1-16 nM) or *E. chrysanthemi* ASNase (0.0625-1 U/mL) or the combination of the two drugs (16:1) or vehicle for 48 h.

Cell viability

Cell viability was assessed by adding resazurin (44 µM) to the incubation media.[38] After 1 h, fluorescence was measured at 572 nm with a fluorimeter (EnSpire® Multimode Plate Readers, Perkin Elmer, Boston, MA, USA). Synergy between *E. chrysanthemi* ASNase and Bortezomib was quantified by combination index analysis using CompuSyn software version 1 (http://combosyn.com/).

NH_4^+ quantification

The quantification of NH_4^+ was detailed in Supplementary Materials and Methods.

From www.bloodjournal.org by guest on July 26, 2016. For personal use only.

Amino acid determination

BM plasma samples were de-proteinized with 10% (w/v) 5-sulfosalicylic acid and centrifuged at 12000*g* for 10 min at 4 °C. Supernatants were mixed with 1 volume of LiOH-citrate buffer (pH 2.2), and the intracellular content of amino acids was determined by HPLC analysis with a Biochrom 20 amino acid analyzer (Amersham Pharmacia Biotech, GE Healthcare Europe GmbH, Milan, Italy), as previously described.[39]

Analysis of the transcriptional profile of glutamine transporters

The analysis of the transcriptional profile of glutamine transporters was described in Supplementary Materials and Methods.

Real time-PCR analysis

Total cell RNA (1 µg), isolated with GenElute™ total RNA Miniprep Kit (Sigma-Aldrich), was reverse transcribed as described.[25] Gln-related enzyme and transporter mRNA expression was analyzed by real-time PCR with the primers reported in Table S2. Data analysis was made according to the Relative Standard Curve Method.[42] The mRNA expression of GAC and KGA was evaluated by taqman gene assay (Life Technologies, Thermo Fisher Scientific, Waltham, MA, USA) by the probes hs01022166_m1 and hs01014019_m1, respectively.

Glutamine uptake

The influx of Gln was measured in RPMI 8226 cells following the method for amino acid transport determination previously described.[43]

Liquid chromatography tandem mass spectrometry (LC-MS/MS)

Cells were seeded in a 6-well plate. After 24 h, growth medium was substituted with fresh medium with or without Gln (4 mM). After 19 h cells were washed with ice-cold Phosphate Buffered Saline, and metabolites were extracted with 1 mL ethanol. LC analyses were carried out with an Agilent HP 1100 pump coupled with a API4000 triple-quadrupole mass spectrometer (AB SCIEX, Framingham, MA, USA) equipped with a TurboIonSpray™ interface and configured in Selected Reaction Monitoring (SRM) mode adapting a previously published method.[44]

From www.bloodjournal.org by guest on July 26, 2016. For personal use only.

Immunoblotting

Immunoblotting analysis was performed as previously described.[35] Blots were incubated at 4 °C overnight with the following antibodies: anti-β-actin (mouse, monoclonal, 1:5000, Sigma-Aldrich) anti-ASCT2 (rabbit, monoclonal, 1:4000, Cell Signaling Technology, Danvers, MA), anti-β-tubulin (mouse, polyclonal, 1:1000, Santa-Cruz Biotechnology, Santa Cruz, CA), anti-caspase 3 (mouse, monoclonal, 1:167, Active Motif, La Hulpe, Belgium), anti-GAPDH (rabbit, polyclonal, 1:4000, Sigma-Aldrich), anti-GLS1 (rabbit, monoclonal, 1:1000, Abcam, Cambridge, UK), anti-GLS2 (rabbit, polyclonal, 1:1000, Abcam), anti-GS (mouse, monoclonal, 1:1500, BD Transduction Laboratories, Franklin Lakes, NJ), anti-LAT1 (rabbit, polyclonal, 1:1000, Cell Signaling Technology), anti-p70S6K, p-T389 (rabbit, monoclonal, 1:1000, Cell Signaling), anti-SNAT1 (rabbit, polyclonal, 1:500, Abcam).

Flow cytometry analysis of apoptosis

$1x10^6$ HMCLs were treated for 24 h under the conditions detailed in the legends to Figures 3 and 4. After the experimental treatments, cells were incubated in the dark with anti-human Apo 2.7-PE (clone 2.7A6A3, Beckman Coulter, Milan, Italy) for 30 min, washed, and then analyzed using FACSCalibur (Becton Dickinson Biosciences (BD) Italia, Milan, Italy).

Lentiviral infection and ASCT2 knockdown

Lentivirus short hairpin RNA (shRNA) anti-*SLC1A5* (Origene, Rockville, MD) was used for ASCT2 stable knockdown in RPMI 8226 and JJN3 cell lines, whereas the scramble lentiviral vector was used as control. Recombinant lentivirus was produced by transient transfection of 293T cells following a standard protocol. HMCLs were infected as previously described,[35] and the efficiency of the infection was evaluated as % of positive cells for green fluorescence protein (GFP) signal by flow cytometry.

In vivo experiments

Severe combined immunodeficiency/non obese diabetic (SCID-NOD) mice (Harlan Laboratories, Udine, Italy) were housed under specific pathogen-free conditions. All procedures involving animals were performed in accordance with the National and International current regulations. 8

From www.bloodjournal.org by guest on July 26, 2016. For personal use only.

mice for group were injected subcutaneously with $5x10^6$ JJN3 cells stably transfected with anti-*SLC1A5* containing plasmid vectors (ΔASCT2) or with the empty vector (Scramble). Tumor growth was monitored at different time points, and 21 days after inoculation mice were sacrificed and autopsies performed. Tumor mass was measured as previously described.[45] Plasmacytomas obtained from tumors removed from mice injected with JJN3 anti-*SLC1A5* or JJN3 scramble were either fixed in 10% neutral buffered formalin, embedded in paraffin, and stained with hematoxylin and eosin, or lysed for protein extraction and western blot analysis.

From www.bloodjournal.org by guest on July 26, 2016. For personal use only.

RESULTS

Myeloma cells produce NH_4^+ from glutamine

Firstly, we assessed the NH_4^+ production by several HMCLs (RPMI 8226, OPM2, JJN3, KMS-12-BM, and XG1) and found that all these lines markedly increased NH_4^+ output in the presence of Gln (Figure 1A). Conversely, the ALL 697 cell line did not (Figure 1A). Primary BM $CD138^+$ PCs from MM patients produced higher NH_4^+ than BM $CD138^-$ cell fraction from the same patients, as shown for 10 representative MM patients (Mann-Whitney test, *P*=.0002 in the presence of Gln, Figure 1B). NH_4^+ production was Gln-dependent (*P*<.0001 for $CD138^+$ fraction, Figure 1B). Comparing NH_4^+ production between HMCLs and primary $CD138^+$ PCs, we found that the Gln-dependent NH_4^+ production was higher in HMCLs (*P*=.0027, Figure 1B). Interestingly, we found that normal PCs obtained from 2 controls produced NH_4^+ in the presence of Gln at lower levels than MM cells, although the difference did not reach statistical significance (normal PCs: median level: 129.1 µmol/L; primary MM cells: 292.6 µmol/L; *P*=0.09).

Higher NH_4^+ levels characterized MM patients as compared to SMM and MGUS

We screened both PB and BM $NH4^+$ levels in subgroups of MM patients and controls. Among 21 MM out of the total cohort of patients enrolled in the study, we showed that 38% of them had high PB NH_4^+ levels (standard limits 10-50 µmol/L) and 14% showed neurological symptoms of encephalopathy without signs of liver dysfunction. In the BM plasma, NH_4^+ levels were significantly higher in patients with active MM as compared with MGUS and SMM (*P*=.042) (Figure 1C). Patients with adverse FISH showed significantly higher BM NH_4^+ levels than the others (median levels 163 µmol/L *versus* 93.5 µmol/L; *P*=.006). Interestingly, BM plasma of MM patients had lower Gln and higher Glu as compared with that of MGUS and SMM patients (Figure 1D and 1E), pointing to glutaminase activity as the responsible of NH_4^+ production. Amino acid profile in BM plasma is reported in Table S3.

On the other hand, no significant correlation between the NH_4^+ levels and % of BM PCs was found (*Pearson* r^2=0.1588, *P*=NS) (data not shown). This observation was further confirmed in another

From www.bloodjournal.org by guest on July 26, 2016. For personal use only.

retrospective cohort of 35 patients with monoclonal gammopathy (*Pearson* r^2=0.0817, *P*=NS) (data not shown).

MM cells express high levels of Glutaminase but not of Glutamine Synthetase

The expression of the two main enzymes responsible for Gln metabolism, Glutaminase-1 (GLS1) and Glutamine Synthetase (GS), was evaluated in five HMCLs and in the ALL 697 cells (Figure 2A). Among the five HMCLs, XG1 had the highest expression of GLS1 (total, KGA, GAC), while the other four cell lines expressed GLS1 mRNAs at levels comparable with those exhibited by ALL cells. Total GLS1 expression and that of the two isoforms GAC and KGA were also detected in primary BM $CD138^+$ cells purified from patients with different monoclonal gammopathies, without any significant difference among the groups (Figure 2B). Comparable levels of GLS1 mRNA were found in normal PCs (data not shown). On the contrary, GLS2 is expressed at very low levels in both HMCLs and primary MM cells (Figure S1). The mRNA of *GLUL*, the gene that encodes for GS, was much less expressed in the five HMCLs than in 697 cells (Figure 2A). HMCLs, with the exception of JJN3 cells, expressed *ASNS*, the gene for Asparagine Synthetase, at higher levels than 697 ALL cells (Figure 2A).

All the HMCLs tested showed similar levels of GLS1 protein, with two clearly detectable enzyme bands (the higher for native KGA and the lower for the cleaved form GAC) (Figure 2C). On the contrary, GS was not detectable in HMCLs but was readily found expressed in 697 cells (Figure 2C). Consistent with mRNA data, ASNS was present in the lysates of all the HMCLs tested at levels comparable (JJN3) or higher than those expressed by ALL 697 cells (Figure 2C). In several cell models, the abundance of GS (protein) is inversely correlated with Gln availability;[46-48] therefore, it is expected that GS will increase when cells are incubated under conditions of Gln shortage. However, even upon incubation in the absence of Gln, GS remained undetectable in HMCLs, while it was much more expressed in Gln-starved ALL cells compared with Gln–fed counterparts (Figure 2D).

GLS1 expression (both KGA and GAC) was also clearly evident in all but one lysates of $CD138^+$ cells from SMM, ND-MM and R-MM patients (Figure 2E). Conversely, GS expression was barely or not detectable at all in the same samples (Figure 2E).

From www.bloodjournal.org by guest on July 26, 2016. For personal use only.

MM cells are dependent on extracellular glutamine and use glutamine for anaplerosis

The high expression detected in MM cells prompted us to evaluate the effects of GLS1 inhibition on cell viability. The GLS1 inhibitor BPTES[49] significantly lowered cell viability in all the HMCLs tested (Figure 3A), with an effect ranging from 30% for JJN3 to 70% for XG1 cells at the highest dose tested (40 µM). Another GLS1 inhibitor, CB-839 (0.125-1 µM), markedly suppressed viability in RPMI 8226 cultures, while it had only small effects in OPM2, KMS-12-BM and XG1 cells and was ineffective in JJN3 cells (Figure 3B).

The low levels of GS expression detected in MM cells support the hypothesis that MM Gln metabolism depends on the availability of the extracellular amino acid. Indeed, when incubated in media at decreasing levels of Gln, HMCLs exhibited a progressive loss of viability; in the absence of the amino acid, viability suppression was complete for RPMI 8226, OPM2 and XG1 lines and >90% for JJN3 and KMS-12-BM cells (Figure 3C). Methionine-sulfoximine (MSO), an irreversible inhibitor of GS, had no effect, thus excluding a protective role of GS in MM cells (Figure 3C).

In order to understand the mechanism involved in the loss of viability of MM cells upon Gln depletion, we tested if Gln had an anaplerotic role in MM cells. To this aim, the intracellular levels of Gln, Glu, and 2-oxoglutarate (2-OG) were measured with mass spectrometry (Figure 3D), demonstrating that Gln-free incubation caused a substantial decrease of the three metabolites. A marked depletion of intracellular Glu and 2-OG, along with an increase of intracellular Gln, was also observed upon cell treatment with the GLS1 inhibitors BPTES and CB-839 (Figure S2). As shown in Figure 3E, Gln depletion caused a significant increase in the percentage of apoptotic cells (P=.014) which was partially mitigated in the presence of a membrane-permeant form of 2-OG (Figure 3E). The anaplerotic role of Gln in MM cells and the related protection by 2-OG were confirmed incubating RPMI 8226, OPM2, JJN3, KMS-12-BM and XG1 cells under conditions of Gln repletion or depletion in the absence or in the presence of 2-OG (Figure 3F). In all the HMCLs, the anaplerotic substrate partially rescued cell viability from the effects of Gln depletion (Figure 3F).

From www.bloodjournal.org by guest on July 26, 2016. For personal use only.

A significant dose-response inhibitory effect on HMCLs proliferation was also observed in the presence of ASNase (Figure 4A). Interestingly, for the five HMCLs tested the IC_{50} values obtained were about ten-fold higher for the *E. coli* than for the *E. chrysanthemi* enzyme (Figure 4A), which is known to have a glutaminolytic activity approximately ten-fold higher compared to the *E. coli* form. Treatment with ASNase caused a massive decrease of cell Gln, but not of intracellular leucine (Figure S3), and led to a marked inhibition of mTOR activity (Figure S4).

Moreover, *Erwinia* ASNase effect on HMCLs viability was increased in the presence of bortezomib (Figure 4B). A synergistic effect was obtained for concentrations of bortezomib lower than 9.3 nM and of ASNase lower that 0.35 U/mL, as shown for RPMI 8226 in Figure 4C. *Erwinia* ASNase significantly reduced cell viability also in bortezomib-resistant RPMI-R5 cells without restoring sensitivity to bortezomib (data not shown).

Finally, the effect on HMCL apoptosis of GLS1 inhibitors, ASNase and bortezomib was investigated in RPMI 8226 and JJN3 cells. In line with the effects on viability, a significant increase in the percentage of apoptotic cells was found in cells treated with BPTES, CB-839 (only for RPMI 8226 cells), *Erwinia* ASNase (alone or in combination with bortezomib) (Figure 4D). The induction of apoptosis in treated cells was also confirmed by the increase of the cleaved Caspase 3 forms (Figure 4E).

MM cells and HMCLs overexpressed glutamine transporters

The dramatic effect of extracellular Gln depletion and ASNase on MM cell viability suggests that the transport of Gln from the extracellular compartment is essential for MM cells. Gln uptake is due to several transporters in human cells.[23] Therefore, the gene expression profiles of some selected Gln transporters were evaluated in two independent PC dyscrasia datasets, both obtained either from proprietary or publicly available databases, including highly purified PC samples throughout the different MM disease phases from the pre-malignant monoclonal gammopathy up to PCL patients, besides healthy donors and HMCLs.

Among the Gln transporters, three carriers known to mediate Gln influx, the Na^+-independent transporter LAT1 and the Na^+-dependent transporters SNAT1 and ASCT2, coded by *SLC7A5*, *SLC38A1* and *SLC1A5*, respectively, showed a significantly increasing trend in expression levels

From www.bloodjournal.org by guest on July 26, 2016. For personal use only.

from normal PCs to HMCLs across the different PC dyscrasias, in both the datasets (Figures 5A and 5B, Tables S4 and S5). Interestingly, the expression of *SNAT1* was also positively correlated with that of *MYC* (*P*=3.965e-12, r=.373; *P*=1.835e-4, r=.22, respectively). $ATB^{0,+}$, another transporter involved in Gln transport in other cell models, coded by *SLC6A14*, did not present consistent changes in expression. SN1 and SN2 (coded by, respectively, *SLC38A3* and *SLC38A5*), two sodium-dependent, lithium-tolerant systems able to mediate bi-directional fluxes of Gln, exhibited a different behavior. SN1 showed lower expression in SPCL and HMCL groups (Figures 5A and 5B, Tables S3 and S4), while SN2, assessed only in one of the datasets, did not show significant changes in MM compared with the other groups.

Two other amino acid transporters, not directly responsible for Gln uptake, also showed significant changes in both the datasets. In particular, xCT (*SLC7A11*) increased from normal PCs to HMCLs. Conversely, y+LAT1 (*SLC7A7*), the low expression of which has been recently described as associated to favorable outcome,[50] had an opposite trend (Figures 5A and 5B, Tables S3 and S4).

MM cells mainly depend on ASCT2 for glutamine transport

On the basis of the gene expression profiling data, we focused our attention on the transporters potentially involved in Gln transport in HMCLs. Preliminarily, we excluded that SN1 or SN2 played a significant role in Gln influx in HMCLs. Although SN2 seems more expressed than SN1 in HMCLs, the overall contribution of the two systems to Gln influx was at best marginal, since lithium did not appreciably stimulate the uptake of Gln in the absence of sodium (Figure S5). Also $ATB^{0,+}$ did not seem to contribute to Gln uptake in HMCLs, since the expression of *SLC6A14* was exceedingly low compared to human airway Calu-3 cells used as a positive control, and, consistently, the preferential substrate D-Ser did not affect significantly Gln influx in MM cells. (Figure S5).

On the contrary, SNAT1, ASCT2 and LAT1 were clearly expressed in all the HMCLs tested at both mRNA (Figure 6A) and protein levels (Figure 6B). The contribution of these transporters to Gln uptake was estimated in RPMI 8226 cells assessing the effects of amino acid analogues (MeAIB, GPNA and BCH), which work as preferential inhibitors of Gln uptake through, respectively, SNAT1, ASCT2 and LAT1 (Figure 6C). Only GPNA caused a marked inhibition of Gln uptake (-60%)

From www.bloodjournal.org by guest on July 26, 2016. For personal use only.

(Figure 6C). The possibility that ASCT2 inhibition could be due to the products of GPNA hydrolysis glutamate and p-nitrophenol has been excluded, demonstrating that, at concentrations markedly larger than those expected during the assay period, the two compounds are without significant effects on Gln uptake (Figure S6). ASCT2 expression was also examined in lysates from $CD138^+$ cells of SMM and MM patients (Figure 6D). The transporter was detected in all the samples, and a trend of higher transporter expression was found in R-MM (Figure 6D). *ASCT2* mRNA was also expressed by normal PCs at similar level of $CD138^+$ cells obtained from patients with monoclonal gammopathies (data not shown).

The activity of ASCT2 is needed for MM growth

To evaluate the effects of Gln transporters on MM cell growth, the transport inhibitors were added to the culture medium of MM cells at the same concentrations used for the inhibition of Gln uptake (Figure 7A). GPNA had the largest growth inhibitory effect, roughly corresponding to a 70%-loss of cell viability compared with untreated control. Also BCH produced a marked decrease in MM cell viability (>50%), while the SNAT1 inhibitor MeAIB produced only a minimal effect.

To assess the effects of ASCT2 silencing on MM cell viability, a lentiviral vector was employed to transfect RPMI 8226 and JJN3 cells with an anti-*SLC1A5* shRNA. A marked repression (>80%) of the transporter expression was obtained at both mRNA and protein level in silenced cells compared with cells transfected with the scramble control (Figures 7B and 7C). Gln influx was substantially lower in ASCT2-silenced than in scramble-transfected cells (Figure 7D). Moreover, the portion of Gln transport inhibited by GPNA was markedly smaller in ASCT2-silenced than in control cells, indicating that the different transport rates were effectively due to ASCT2 silencing. Compared with the scramble-transfected control, both ASCT2-silenced (ΔASCT2) RPMI 8226 and JJN3 cells exhibited a lower growth (two-tailed t test, RPMI 8226 ΔASCT2 *versus* RPMI 8226 Scramble $P=3.9\text{x}10^{-9}$; JJN3 ΔASCT2 *versus* JJN3 Scramble $P=.0002$) (Figure 7E). Either by flow cytometry (Apo 2.7 staining) and western blotting (Caspase 3 activation), we did not obtain clear cut signs of cell death/apoptosis induced by ASCT2 silencing (data not shown). Although statistical significance was not reached, ASCT2-silenced cells exhibited a trend to consume less Gln than control cells (Figure S7).

From www.bloodjournal.org by guest on July 26, 2016. For personal use only.

Stable ASCT2 silencing inhibited MM growth in vivo

Finally, to confirm *in vivo* our *in vitro* evidence, we investigated whether the silencing of ASCT2 influences MM cell tumor growth in a murine xenograft model. To this purpose, JJN3 cells, transfected with the anti-ASCT2 shRNA (ΔASCT2) or with the scramble control (Scramble), were injected subcutaneously into SCID-NOD animals. As shown in Figure 7F, mice inoculated with the ASCT2-silenced cells developed significantly smaller tumors than animals injected with the scramble-transfected cells. A significant reduction of the tumor size was confirmed after plasmacytoma explant and hematoxylin-eosin staining, as shown for two representative mice (Figure 7G). At the sacrifice, the expression of ASCT2 was markedly lower in ΔASCT2 than in scramble-transfected tumors, as confirmed by western blot (Figure 7H).

From www.bloodjournal.org by guest on July 26, 2016. For personal use only.

DISCUSSION

Hyperammonemia has been reported as a possible feature of MM patients.[7-12] Single cases have been described in the literature and retrospective screening of the database of MM patients. Otsuki *et al.* found that 60% of 20 patients died for MM had high serum NH_4^+ levels, although data on liver function and the presence of encephalopathy were not reported.[4] On the other hand, Matsuzaki *et al.* reported that 7% of 85 patients had hyperammonemia associated with neurological signs.[7] Similarly, the Arkansas group found 3.8% of 209 patients with hyperammonemia and encephalopathy, without liver dysfunction.[10] In our prospective cohort of MM patients, we show that about 38% of 21 patients analyzed, without liver dysfunction, had high peripheral NH_4^+ levels, but only 14% with signs of encephalopathy. Despite of the differences observed in the prevalence of hyperammonemia, attributable to the different series of patients analyzed or, as recently reported, by the high technical variability in testing serum NH_4^+ levels,[51] overall, these observations support the hypothesis that MM cells may produce NH_4^+. In fact, while excess NH_4^+ production by HMCLs has been demonstrated *in vitro*,[5,4] the mechanisms involved, and the possible relationship with the dependence of their growth on Gln,[3] have not been investigated.

In this study, firstly, we show that not only HMCLs but also $CD138^+$ PCs from MM patients produce NH_4^+ from Gln. Indeed, analyzing BM plasma NH_4^+ levels in different cohorts of patients with monoclonal gammopathies, we show that MM patients had significant higher levels than those with SMM and MGUS, without a significant relationship with the number of BM PCs. Higher NH_4^+ was associated with higher Glu and lower Gln levels, which indicates that neoplastic PCs exert active glutaminolysis *in vivo*. Accordingly, expression of GLS1 is consistently present in HMCLs and detected in primary $CD138^+$ cells from almost all MM patients. Secondly, we demonstrate that Gln represents an absolute nutritional requirement for neoplastic PCs, and that these cells, lacking a detectable expression of GS, exclusively rely on the uptake of extracellular Gln to satisfy their needing for the amino acid. This is consistent with high sensitivity of HMCLs to the depletion of extracellular Gln and to the silencing/inhibition of the Gln transporter ASCT2.

From www.bloodjournal.org by guest on July 26, 2016. For personal use only.

Although the sensitivity shown by each HMCL towards BPTES and CB389 is different, glutaminase inhibitors also hinder HMCL cell growth and induced apoptosis, suggesting that glutaminolysis has an important role in MM cell metabolism. Through glutaminolysis, Gln replenishes the intracellular pool of Glu and, through transaminases and Glu dehydrogenase, of the Krebs cycle intermediate 2-OG, thus playing an anaplerotic role. As shown in several human cancer models,[18,23,52,53] Gln-dependent anaplerosis is one of the mechanisms likely underlying Gln addiction, which implies the needing for large amounts of the amino acid. The anaplerotic role of Gln in MM cells, and the Gln addiction of this cancer model, is confirmed by the fall in 2-OG levels observed in Gln-depleted cells and by the rescue of Gln-depleted myeloma cells observed upon medium supplementation with the membrane-permeant analogue dimethyl-2-OG. However, viability rescue from 2-OG is only partial, indicating that, besides anaplerosis, Gln plays other pro-survival roles in MM cells. Indeed, while 2-OG easily supplies the intracellular Glu pool, the conversion of Glu to Gln is still prevented in MM cells by the absence of GS. Consequently, all the pathways that exhibit an absolute requirement for Gln will be severely hampered if a GS-negative MM cell is incubated under Gln-free conditions. Thus, human MM cells present a thus far unknown association between signs of Gln addiction and lack of expression of GS, two features that synergistically increase the dependence of MM cells upon extracellular Gln.

Consistently, HMCLs are more sensitive to *E. chrysanthemi* ASNase than to the *E. coli* enzyme. While the two enzymes have comparable asparaginolytic activities, they differ as far as Gln hydrolysis is concerned, with the *Erwinia* enzyme endowed with a ten-fold higher activity. Interestingly, the five HMCLs tested exhibited comparable IC_{50} values for *Erwinia* ASNase, although they express Asparagine Synthetase at different levels. Moreover, ASNase caused a massive depletion of intracellular Gln but not of leucine (Figure S3), while markedly inhibited mTOR activity (Figure S4). However, rapamycin had much smaller effects on cell viability than ASNase (Figure S4). Collectively, these data suggest that the hydrolysis of extracellular Gln, followed by the depletion of the intracellular Gln pool, is the prevalent mechanism of the anti-myeloma activity exhibited by ASNase.

From www.bloodjournal.org by guest on July 26, 2016. For personal use only.

These considerations highlight the critical importance that Gln transport assumes for MM cells, as suggested by the changes in gene expression across the progression of human PC dyscrasias. Many transporters are potentially involved in Gln transport.[16,54] However, the contribution of $ATB^{0,+}$ (*SLC6A14*), SN1 (*SLC38A3*) and SN2 (*SLC38A5*), known to interact with Gln in other cell models,[16,54] did not appear important (Figure S5). Three other transporters, LAT1, SNAT1 and ASCT2, showed increased expression during MM progression, suggesting that the affirmation of the neoplastic clone may require a growing supply of the amino acid through their operation. The relative contribution of each transporter to the uptake depends on several factors, the most important of which is the affinity towards Gln.[16] For this reason, the discrimination of transporter contribution to Gln uptake in MM cells has been performed at a concentration of Gln comparable to that present in human plasma. Under these conditions, ASCT2, estimated from the portion of uptake inhibited by GPNA, accounts for most of Gln influx, with SNAT1 and LAT1 restricted to minor roles. Consistently, GPNA suppressed MM cell viability. However, growth inhibition by the LAT1 inhibitor BCH was much larger than its effect on Gln uptake. This apparent anomaly may be explained considering that LAT1 also mediates the influx of many essential amino acids.

After showing that also ASCT2 silencing *in vitro* had significant inhibitory effects on MM cell growth in two different HMCLs, we confirmed these results with a xenograft model, although tumor growth inhibition was only partial. This result, comparable to data obtained with similar approaches in other human cancer models,[15,23,27] suggests that, when faced with scarce Gln fluxes from the extracellular compartment, MM cells can adopt escaping strategies based on the operation of other transporters. A good candidate could be the SNAT1 transporter, which, although found overexpressed in the genome-wide expression analysis during MM progression and nicely expressed in HMCLs, seems to account for a very minor portion of Gln uptake under control (Gln repleted) conditions. *SLC7A11* gene has been also found overexpressed in MM cells. This gene encodes for xCT, an important transporter needed for exchanging intracellular Glu and extracellular cystine, which is involved in the cell response to oxidative stress.[55]

Finally, our data indicate that blocking Gln uptake could be, possibly in association with other approaches, a suitable target to inhibit MM cell growth as also reported for other haematological

From www.bloodjournal.org by guest on July 26, 2016. For personal use only.

malignancies.[23,24,27] In line with this hypothesis, we show that bortezomib increased the cytotoxic effect of *E. chrysanthemi* ASNase as previously reported for acute leukemia cells.[56]

Others recently showed that CB-839 blocks MM growth and synergized with pomalidomide in preclinical model,[57] and a phase I trial with CB-839 in patients with R-MM is currently under investigation.[58] Moreover, it has been recently reported that Gln withdrawal enhanced MM cell sensitivity to BH3 mimetics venetoclax (ABT-199), a new anti-myeloma drug currently under investigation[59], and that ritonavir increases the Gln reliance of MM cells.[60] Overall, these data and our results suggest that Gln addiction and uptake could be a potential new therapeutic strategy in MM patients.

From www.bloodjournal.org by guest on July 26, 2016. For personal use only.

Acknowledgements

We thank Dirce Gennari for her technical support.

This work was supported in part by a grant from the Associazione Italiana per la Ricerca sul Cancro IG2014 n.15531 (N.G.), AIRC IG n.13018 (I.A.), and a fellowship Fondazione Italiana per la Ricerca sul Cancro id. 18152 (M.B.).

Authorship

M.B. and M.C. performed all the *in vitro* experiments, supported by M.G.B., M.A., A.B., D.T., F.C. and V.M. R.A. performed the LC-MS analysis. F.A., O.B. and N.G. designed the study. M.B., M.C., O.B. and N.G. analyzed data and wrote the manuscript. F.A., F.N. and N.G. provide clinical data and patients. I.A. performed the *in vivo* studies, R.V. generated the flow cytometry data and G.D. designed the lentiviral approach. K.T. and L.A. generated the gene expression profile analyses. G.M. and A.C. were responsible for ammonium quantification. C.M. and E.M. performed the histological analysis. M.B., M.C., F.A., P.S., O.B. and N.G. were involved in the interpretation of the results. V.D.A. and F.A. read, provided comments, and approved the final version of the manuscript.

Conflicts of Interests

The research fellowship of M.C. is partially supported by a grant of Jazz Pharmaceuticals Ltd. to O.B.

From www.bloodjournal.org by guest on July 26, 2016. For personal use only.

REFERENCES

1. Anderson KC. Multiple myeloma. *Hematol Oncol Clin North Am*. 2014;28(5):xi-xii.
2. Palumbo A, Anderson K. Multiple myeloma. *N Engl J Med*. 2011;364(11):1046-1060.
3. Roberts PJ. Amino acid transport in spinal and sympathetic ganglia. *Adv Exp Med Biol*. 1976;69:165-178.
4. Otsuki T, Yamada O, Sakaguchi H, et al. In vitro excess ammonia production in human myeloma cell lines. *Leukemia*. 1998;12(7):1149-1158.
5. Matsuzaki H, Matsuno F, Yoshida M, Hata H, Okazaki K, Takatsuki K. Human myeloma cell line (KHM-4) established from a patient with multiple myeloma associated with hyperammonemia. *Intern Med*. 1992;31(3):339-343.
6. Lora-Tamayo J, Palom X, Sarra J, et al. Multiple myeloma and hyperammonemic encephalopathy: review of 27 cases. *Clin Lymphoma Myeloma*. 2008;8(6):363-369.
7. Matsuzaki H, Hata H, Sonoki T, et al. Serum amino acid disturbance in multiple myeloma with hyperammonemia. *Int J Hematol*. 1995;61(3):131-137.
8. Kwan L, Wang C, Levitt L. Hyperammonemic encephalopathy in multiple myeloma. *N Engl J Med*. 2002;346(21):1674-1675.
9. Furer V, Heyd J. Hyperammonemic encephalopathy in multiple myeloma. *Isr Med Assoc J*. 2007;9(7):557-559.
10. Talamo G, Cavallo F, Zangari M, et al. Hyperammonemia and encephalopathy in patients with multiple myeloma. *Am J Hematol*. 2007;82(5):414-415.
11. Benet B, Alexandra JF, Andrieu V, Sedel F, Ajzenberg N, Papo T. Multiple myeloma presenting as hyperammonemic encephalopathy. *J Am Geriatr Soc*. 2010;58(8):1620-1622.
12. Pham A, Reagan JL, Castillo JJ. Multiple myeloma-induced hyperammonemic encephalopathy: an entity associated with high in-patient mortality. *Leuk Res*. 2013;37(10):1229-1232.
13. Puchades-Carrasco L, Lecumberri R, Martinez-Lopez J, et al. Multiple myeloma patients have a specific serum metabolomic profile that changes after achieving complete remission. *Clin Cancer Res*. 2013;19(17):4770-4779.
14. Adeva MM, Souto G, Blanco N, Donapetry C. Ammonium metabolism in humans. *Metabolism*. 2012;61(11):1495-1511.
15. Wise DR, Thompson CB. Glutamine addiction: a new therapeutic target in cancer. *Trends Biochem Sci*. 2010;35(8):427-433.
16. Pochini L, Scalise M, Galluccio M, Indiveri C. Membrane transporters for the special amino acid glutamine: structure/function relationships and relevance to human health. *Front Chem*. 2014;2:61.
17. Durand P, Golinelli-Pimpaneau B, Mouilleron S, Badet B, Badet-Denisot MA. Highlights of glucosamine-6P synthase catalysis. *Arch Biochem Biophys*. 2008;474(2):302-317.
18. Tanaka K, Sasayama T, Irino Y, et al. Compensatory glutamine metabolism promotes glioblastoma resistance to mTOR inhibitor treatment. *J Clin Invest*. 2015;125(4):1591-1602.
19. Yang L, Moss T, Mangala LS, et al. Metabolic shifts toward glutamine regulate tumor growth, invasion and bioenergetics in ovarian cancer. *Mol Syst Biol*. 2014;10:728.
20. Ratnikov B, Aza-Blanc P, Ronai ZA, Smith JW, Osterman AL, Scott DA. Glutamate and asparagine cataplerosis underlie glutamine addiction in melanoma. *Oncotarget*. 2015;6(10):7379-7389.
21. Fogal V, Babic I, Chao Y, et al. Mitochondrial p32 is upregulated in Myc expressing brain cancers and mediates glutamine addiction. *Oncotarget*. 2015;6(2):1157-1170.
22. Tardito S, Chiu M, Uggeri J, et al. L-Asparaginase and inhibitors of glutamine synthetase disclose glutamine addiction of beta-catenin-mutated human hepatocellular carcinoma cells. *Curr Cancer Drug Targets*. 2011;11(8):929-943.
23. Bhutia YD, Babu E, Ramachandran S, Ganapathy V. Amino Acid transporters in cancer and their relevance to "glutamine addiction": novel targets for the design of a new class of anticancer drugs. *Cancer Res*. 2015;75(9):1782-1788.

From www.bloodjournal.org by guest on July 26, 2016. For personal use only.

24. Hassanein M, Hoeksema MD, Shiota M, et al. SLC1A5 mediates glutamine transport required for lung cancer cell growth and survival. *Clin Cancer Res*. 2013;19(3):560-570.
25. Chiu M, Tardito S, Pillozzi S, et al. Glutamine depletion by crisantaspase hinders the growth of human hepatocellular carcinoma xenografts. *Br J Cancer*. 2014;111(6):1159-1167.
26. Gross MI, Demo SD, Dennison JB, et al. Antitumor activity of the glutaminase inhibitor CB-839 in triple-negative breast cancer. *Mol Cancer Ther*. 2014;13(4):890-901.
27. Willems L, Jacque N, Jacquel A, et al. Inhibiting glutamine uptake represents an attractive new strategy for treating acute myeloid leukemia. *Blood*. 2013;122(20):3521-3532.
28. Jacque N, Ronchetti AM, Larrue C, et al. Targeting glutaminolysis has antileukemic activity in acute myeloid leukemia and synergizes with BCL-2 inhibition. *Blood*. 2015;126(11):1346-1356.
29. Sugimoto K, Suzuki HI, Fujimura T, et al. A clinically attainable dose of L-asparaginase targets glutamine addiction in lymphoid cell lines. *Cancer Sci*. 2015.
30. Avramis VI. Asparaginases: biochemical pharmacology and modes of drug resistance. *Anticancer Res*. 2012;32(7):2423-2437.
31. Pieters R, Hunger SP, Boos J, et al. L-asparaginase treatment in acute lymphoblastic leukemia: a focus on Erwinia asparaginase. *Cancer*. 2011;117(2):238-249.
32. Chan WK, Lorenzi PL, Anishkin A, et al. The glutaminase activity of L-asparaginase is not required for anticancer activity against ASNS-negative cells. *Blood*. 2014;123(23):3596-3606.
33. Boyd KD, Ross FM, Chiecchio L, et al. A novel prognostic model in myeloma based on co-segregating adverse FISH lesions and the ISS: analysis of patients treated in the MRC Myeloma IX trial. *Leukemia*. 2012;26(2):349-355.
34. Chng WJ, Dispenzieri A, Chim CS, et al. IMWG consensus on risk stratification in multiple myeloma. *Leukemia*. 2014;28(2):269-277.
35. Bolzoni M, Donofrio G, Storti P, et al. Myeloma cells inhibit non-canonical wnt co-receptor ror2 expression in human bone marrow osteoprogenitor cells: effect of wnt5a/ror2 pathway activation on the osteogenic differentiation impairment induced by myeloma cells. *Leukemia*. 2013;27(2):451-463.
36. Palma BD, Guasco D, Pedrazzoni M, et al. Osteolytic lesions, cytogenetic features and bone marrow levels of cytokines and chemokines in multiple myeloma patients: Role of chemokine (C-C motif) ligand 20. *Leukemia*. 2015.
37. Buzzeo R, Enkemann S, Nimmanapalli R, et al. Characterization of a R115777-resistant human multiple myeloma cell line with cross-resistance to PS-341. *Clin Cancer Res*. 2005;11(16):6057-6064.
38. O'Brien J, Wilson I, Orton T, Pognan F. Investigation of the Alamar Blue (resazurin) fluorescent dye for the assessment of mammalian cell cytotoxicity. *Eur J Biochem*. 2000;267(17):5421-5426.
39. Dall'Asta V, Bussolati O, Sala R, et al. Amino acids are compatible osmolytes for volume recovery after hypertonic shrinkage in vascular endothelial cells. *Am J Physiol*. 1999;276(4 Pt 1):C865-872.
40. Todoerti K, Agnelli L, Fabris S, et al. Transcriptional characterization of a prospective series of primary plasma cell leukemia revealed signatures associated with tumor progression and poorer outcome. *Clin Cancer Res*. 2013;19(12):3247-3258.
41. Lionetti M, Barbieri M, Todoerti K, et al. Molecular spectrum of BRAF, NRAS and KRAS gene mutations in plasma cell dyscrasias: implication for MEK-ERK pathway activation. *Oncotarget*. 2015;6(27):24205-24217.
42. Bustin SA. Absolute quantification of mRNA using real-time reverse transcription polymerase chain reaction assays. *J Mol Endocrinol*. 2000;25(2):169-193.
43. Bianchi MG, Gazzola GC, Tognazzi L, Bussolati O. C6 glioma cells differentiated by retinoic acid overexpress the glutamate transporter excitatory amino acid carrier 1 (EAAC1). *Neuroscience*. 2008;151(4):1042-1052.
44. Huang Y, Tian Y, Zhang Z, Peng C. A HILIC-MS/MS method for the simultaneous determination of seven organic acids in rat urine as biomarkers of exposure to realgar. *J Chromatogr B Analyt Technol Biomed Life Sci*. 2012;905:37-42.
45. Storti P, Bolzoni M, Donofrio G, et al. Hypoxia-inducible factor (HIF)-1alpha suppression in myeloma cells blocks tumoral growth in vivo inhibiting angiogenesis and bone destruction. *Leukemia*. 2013;27(8):1697-1706.

From www.bloodjournal.org by guest on July 26, 2016. For personal use only.

46. Huang YF, Wang Y, Watford M. Glutamine directly downregulates glutamine synthetase protein levels in mouse C2C12 skeletal muscle myotubes. *J Nutr*. 2007;137(6):1357-1362.
47. Labow BI, Abcouwer SF, Lin CM, Souba WW. Glutamine synthetase expression in rat lung is regulated by protein stability. *Am J Physiol*. 1998;275(5 Pt 1):L877-886.
48. Labow BI, Souba WW, Abcouwer SF. Glutamine synthetase expression in muscle is regulated by transcriptional and posttranscriptional mechanisms. *Am J Physiol*. 1999;276(6 Pt 1):E1136-1145.
49. Robinson MM, McBryant SJ, Tsukamoto T, et al. Novel mechanism of inhibition of rat kidney-type glutaminase by bis-2-(5-phenylacetamido-1,2,4-thiadiazol-2-yl)ethyl sulfide (BPTES). *Biochem J*. 2007;406(3):407-414.
50. Agnelli L, Forcato M, Ferrari F, et al. The reconstruction of transcriptional networks reveals critical genes with implications for clinical outcome of multiple myeloma. *Clin Cancer Res*. 2011;17(23):7402-7412.
51. Howells JW, Short PA. The Importance of Clinical Context When Interpreting Serum Ammonia Levels: A Teachable Moment. *JAMA Intern Med*. 2015;175(12):1902-1903.
52. Kim MH, Kim H. Oncogenes and tumor suppressors regulate glutamine metabolism in cancer cells. *J Cancer Prev*. 2013;18(3):221-226.
53. Katt WP, Cerione RA. Glutaminase regulation in cancer cells: a druggable chain of events. *Drug Discov Today*. 2014;19(4):450-457.
54. Schioth HB, Roshanbin S, Hagglund MG, Fredriksson R. Evolutionary origin of amino acid transporter families SLC32, SLC36 and SLC38 and physiological, pathological and therapeutic aspects. *Mol Aspects Med*. 2013;34(2-3):571-585.
55. Lewerenz J, Maher P, Methner A. Regulation of xCT expression and system x (c) (-) function in neuronal cells. *Amino Acids*. 2012;42(1):171-179.
56. Horton TM, Gannavarapu A, Blaney SM, D'Argenio DZ, Plon SE, Berg SL. Bortezomib interactions with chemotherapy agents in acute leukemia in vitro. *Cancer Chemother Pharmacol*. 2006;58(1):13-23.
57. Parlati F, Gross M, Janes J, et al. Glutaminase Inhibitor CB-839 Synergizes with Pomalidomide in Preclinical Multiple Myeloma Models. *Blood*. 2014;124(21).
58. Vogl DT, Younes A, Stewart K, et al. Phase 1 Study of CB-839, a First-in-Class, Glutaminase Inhibitor in Patients with Multiple Myeloma and Lymphoma. *Blood*. 2015;126(23):3059 - 3059.
59. Bajpai R, Matulis SM, Wei C, et al. Targeting glutamine metabolism in multiple myeloma enhances BIM binding to BCL-2 eliciting synthetic lethality to venetoclax. *Oncogene*. 2015.
60. Dalva-Aydemir S, Bajpai R, Martinez M, et al. Targeting the metabolic plasticity of multiple myeloma with FDA-approved ritonavir and metformin. *Clin Cancer Res*. 2015;21(5):1161-1171.

From www.bloodjournal.org by guest on July 26, 2016. For personal use only.

LEGEND OF FIGURES

Figure 1: MM cells produce ammonium in excess in the presence of Gln.

RPMI 8226, OPM2, JJN3, KMS-12-BM, XG1, and 697 cells were seeded at $5x10^5$ cells/mL in RPMI-1640 with 10% FBS in the presence (w) or absence (w/o) of Gln (4 mM) and cultured for 16 h. CM were collected and immediately analyzed. The CM of primary BM $CD138^+$ and $CD138^-$ fractions of 10 MM patients were also obtained, following the same procedure. Then NH_4^+ levels were evaluated. **(A)** Bar graph represents the mean NH_4^+ plus Standard Deviation (SD) secreted by cell lines in two independent experiments (two-tailed unpaired t test, **P*<.05; ***P*<.01). **(B)** Plots represent the single values of NH_4^+ secreted by HMCLs, BM $CD138^+$ MM cells, and BM $CD138^-$ cells. **(C)** Plots represent the single values of BM plasma NH_4^+ of patients affected by MGUS and SMM (n=13) and by active MM (n=17). **(D)** Gln and **(E)** glutamate (Glu) in BM plasma of patients with indolent monoclonal gammopathies (MGUS and SMM) (n=10) or active MM (n=13), evaluated by HPLC. For **(B-E),** lines represent median values for Mann-Whitney test.

Figure 2: MM cells exhibit high expression of GLS1 but not GS.

(A) GLS1, GAC, KGA, GLUL, and ASNS expression was analyzed by real time-PCR in HMCLs and 697 cells. Gene expression was normalized to the expression of *RPL-15*. GAC/KGA mRNA was also reported. Means plus SD of three experiments with two determinations each are shown. **(B)** GLS1, GAC, and KGA expression in primary $CD138^+$ cells, purified from 3 MGUS, 5 SMM, 11 ND-MM, and 10 R-MM patients, was evaluated with real time-PCR. Lines represent median values. **(C)** Western blot of GLS1, GS, and ASNS expression by HMCLs and 697 cells. β -tubulin was used for loading control. **(D)** GS expression in HMCLs and 697 cells incubated for 19 h in the presence of 4 mM Gln (+) or in the absence of the amino acid (-). **(E)** GLS1 and GS expression was evaluated by western blot in $CD138^+$ cells purified from 4 SMM, 7 ND-MM and 4 R-MM patients. 697 lysate was used as positive control. GAPDH was used for loading control.

From www.bloodjournal.org by guest on July 26, 2016. For personal use only.

Figure 3: MM cells are sensitive to Gln depletion.

(A) HMCLs were treated with increasing concentrations of BPTES or vehicle (-). After 48 h cell viability was assessed and data were expressed as % of the value obtained with cells treated with the vehicle **(B)** HMCLs were treated with increasing concentrations of CB-839 or vehicle (-). After 48 h cell viability was assessed, and data were expressed as % of the value obtained with cells treated with the vehicle **(C)** HMCLs were incubated with decreasing concentrations of Gln in the absence or in the presence of the GS inhibitor MSO (1 mM). After 48 h cell viability was assessed, and data were expressed as % of the cell growth observed at 4 mM Gln. **(D)** Cell contents of Gln, Glu and oxoglutarate (2-OG) were measured by LC-MS/MS in RPMI 8226 incubated for 19 h in the presence (4 mM) or in the absence of Gln. Data were expressed as nmol/mg protein. **(E)** RPMI 8226 were incubated in the presence (4 mM) or in the absence of Gln with or without dimethyl-2-OG (8 mM). After 24 h, the expression of the apoptosis marker Apo 2.7 was checked by flow cytometry. **(F)** MM cells were incubated in the presence (4 mM) or in the absence of Gln with or without dimethyl-2-OG (8 mM). After 48 h cell viability was assessed and data were expressed as % of control (Gln present, 2-OG absent). For **(A-F)**, data are means ± SD of three experiments with three determinations each.*P<.05, ***P<.001 *versus* control.

Figure 4: MM cells are sensitive to *E. chrysanthemi ASNase* treatment.

(A) HMCLs were treated with increasing doses of L-Asparaginase (ASNase) from *E. coli* or *E. chrysanthemi* (from 0.0001 to 1 U/mL). After 48 h, cell viability was assessed, and data were expressed as % of the value obtained with untreated cells. For each HMCL, IC_{50} for *E. coli* ASNase and for the *E. chrysanthemi* enzyme are shown. **(B)** HMCLs were treated with increasing doses of bortezomib (from 1.77 to 10 nM), or vehicle in the presence or in the absence of *E. chrysanthemi* ASNase (0.1 U/mL). After 48 h, cell viability was assessed, and data were expressed as % of the value obtained with the cells treated with vehicle. For **(A-B)**, data are means ± SD of three experiments with three determinations each. **(C)** RPMI 8226 were treated with increasing doses of bortezomib (from 1 to 16 nM), or increasing doses of *E. chrysanthemi* ASNase (from 0.0625 to 1 U/mL), or the combination of the two drugs (16:1), or vehicle. After 48 h, cell viability was

From www.bloodjournal.org by guest on July 26, 2016. For personal use only.

assessed, and the data were analyzed as % of the value obtained with the cells treated with vehicle. Combination index analysis was then performed using CompuSyn software. Isobologram for ED_{75} represents means ± SEM of three experiments with five determinations each. **(D, E)** RPMI 8226 and JJN3 cells were treated for 24 h with BPTES (40 µM), or CB-839 (1 µM), or ASNase from *E. coli* (1 U/ml), or ASNase from *E. chrysanthemi* (0.1 U/ml), or bortezomib (10 nM), or ASNase from *E. chrysanthemi* (0.1 U/ml) and bortezomib (10 nM), or vehicles. For **(D)**, cell expression of Apo 2.7 was then evaluated by flow cytometry. The graph shows the mean % plus SD (n = 3) of Apo 2.7 positive cells for each condition after the subtraction of the value obtained in control. For **(E)**, cells expression of cleaved forms of Caspases 3 in HMCLs, evaluated by western blot. β-Actin was used for loading control. For **(A-B, D)** **P*<.05, ****P*<.001 *versus* control.

Figure 5: Gene expression profiling of the main glutamine transporters by CD138$^+$ cells.

(A) Box plot distribution of the expression levels of *SLC7A5* (LAT1), *SLC1A5* (ASCT2), *SLC38A1* (SNAT1), *SLC6A14* ($ATB^{0,+}$) *SLC7A11* (xCT), *SLC38A3* (SN1) and *SLC7A7 (*y+LAT1) genes in a 323-sample dataset, including 18 healthy donors (N), 28 MGUS, 19 SMM, 200 ND-MM, 26 R-MM, 9 PCL patients, together with 23 HMCLs. This 323-sample dataset was generated using GSE13591, GSE6205, GSE6477 and GSE6691 dataset, profiled on GeneChip® Human Genome U133A Arrays. **(B)** Box plot distribution of the expression levels of the same Gln transporter genes shown in panel (A) plus *SLC38A5* (SN2) in a 283-sample dataset, comprising 9 N, 20 MGUS, 33 SMM and 170 ND-MM, 24 PPCL and 9 SPCL cases, and also including 18 HMCLs. This 283-sample dataset was obtained using GSE66293 and GSE47552 dataset, analyzed on GeneChip® Human Gene 1.0 ST array. For **(A-B),** the significance of Kruskal-Wallis and Jonckheere-Terpstra tests was indicated.

Figure 6: ASCT2 is the major glutamine transporter in MM cells.

(A) *SLC38A1*, *SLC1A5* and *SLC7A5* gene expression in MM cells, incubated in standard growth medium ([Gln] = 4 mM), were analyzed through real time-PCR. Transporter expression in the human hepatocellular carcinoma cell line HepG2 was used as a positive control. Gene expression

From www.bloodjournal.org by guest on July 26, 2016. For personal use only.

was normalized to the expression of *RPL-15*. Means ± SD of three experiments, with two determinations each, are shown. **(B)** SNAT1, ASCT2 and LAT1 expression in HMCLs, incubated in standard growth medium, was analyzed by western blot. HepG2 cells were used as a positive control. β-tubulin was used for loading control. **(C)** 1-Min uptake of L-[3,4-^{3}H(N)] Gln (0.6 mM, 20 µCi/mL, Amersham) by RPMI 8226 was performed in serum-free culture medium in the absence (-) or in the presence of the transport inhibitors α-(methylamino)isobutyric acid (MeAIB, 20 mM), L-γ-glutamyl-*p*-nitroanilide (GPNA, 3 mM), or 2-amino-2-norbornanecarboxylic acid (BCH, 20 mM). Means ± SD of three experiments, with five independent determinations each, are shown. ***P<.001 *versus* control. **(D)** ASCT2 expression was investigated in lysates of the CD138^{+} population isolated from monoclonal gammopathies patients. The same membrane shown in Figure 2E was blotted with anti-ASCT2 antibody.

Figure 7: ASCT2 silencing by lentiviral vector impairs MM cell growth *in vitro* and *in vivo*.

(A) RPMI 8226 cells were incubated in growth medium ([Gln] = 0.6 mM) in the absence (control) or in the presence of MeAIB (20 mM), GPNA (3 mM), or BCH (20 mM). After 72 h, cell viability was assessed, and results were expressed as % of control. Data represent means ± SD of three experiments with three determinations each. **P<.01, ***P<.001 *versus* control as assessed with a two-tail Student's t test for unpaired data. **(B-C)** ASCT2 expression in scramble and ΔASCT2 RPMI 8226 **(B)** and JJN3 cells **(C)**. Gene expression was evaluated with qRT-PCR and normalized to the expression of *RPL-15*. ASCT2 protein expression was evaluated with western blot and β-tubulin was used for loading control. **(D)** 1-Min uptake of Gln (0.6 mM) was performed in scramble and ΔASCT2 RPMI 8226 cells in culture medium in the absence (-) or in the presence of GPNA (3 mM). ***P<.001 *versus* control. $$$$P$<.001 *versus* scramble, as assessed with a two-tail Student's t test for unpaired data. **(E)** Scramble and ΔASCT2 RPMI 8226 and JJN3 cells, both at 5x10^{5} cells/mL, were grown for 72 h in medium at 0.6 mM Gln. Cell growth was monitored at the indicated times with the resazurin assay. Data represent means ± SD of two experiments with three determinations each. SD are shown when greater than the size of the point. **(F-G-H)** Two groups of 8 SCID/NOD animals each were injected subcutaneously with 5x10^{6} JJN3 cells

From www.bloodjournal.org by guest on July 26, 2016. For personal use only.

transfected with a lentiviral vector containing shRNA against ASCT2 (ΔASCT2) or with the control vector (Scramble). Twenty-one days after cell inoculation, mice were killed, and tumors were removed and measured as described in the Patients, Materials and Methods section. **(F)** The box plot graph represents the median volume of the masses. (*P* calculated by Mann-Whitney test). **(G)** Representative picture of tumors obtained from mice injected with JJN3 Scramble and ΔASCT2 cells stained with hematoxylin-eosin (Original magnification 1x). **(H)** ASCT2 expression was assessed in plasmacytomas removed after animal sacrifice. β-tubulin was used for loading control.

Figure 1

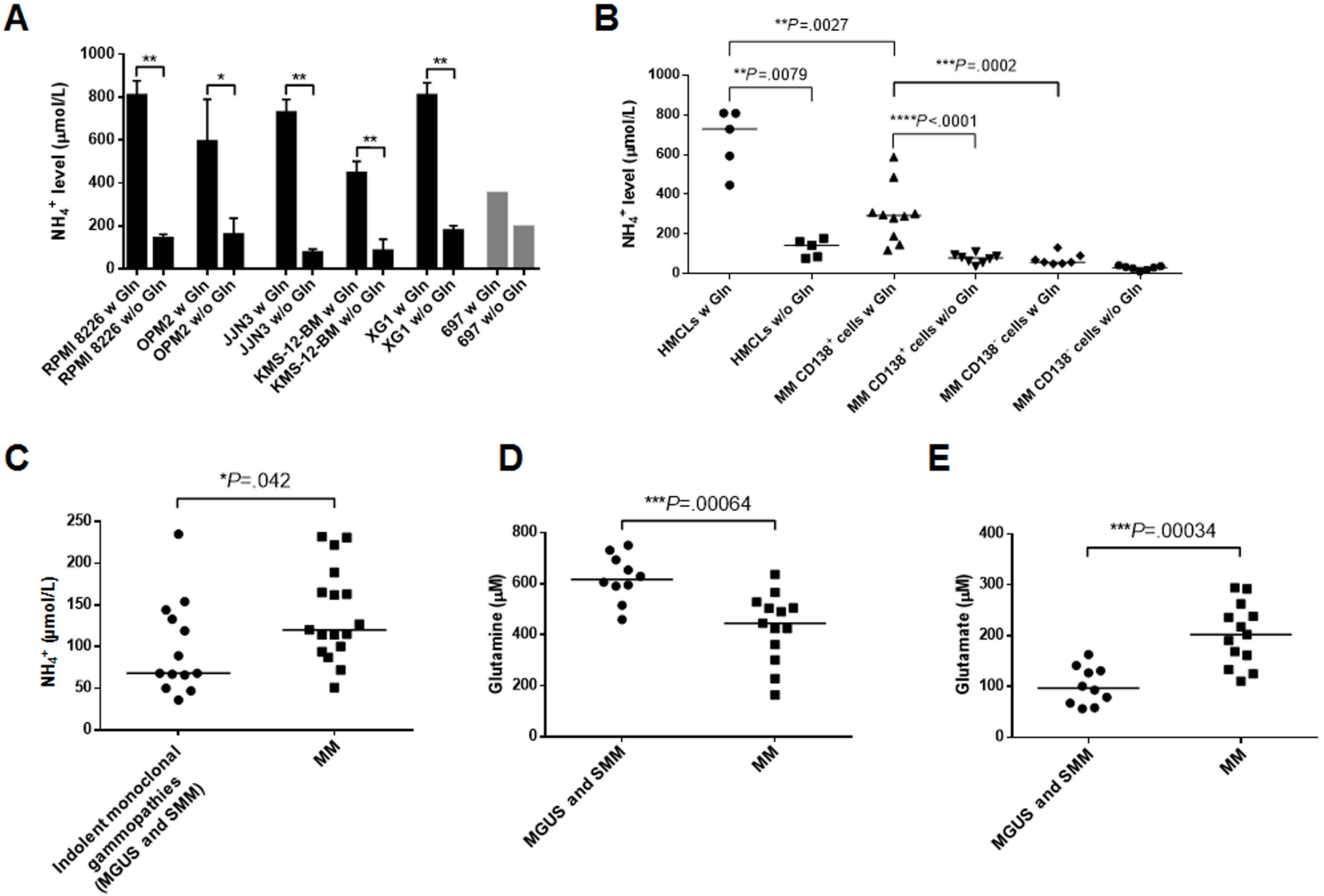
A
1000
800
600
400
200
0
NH_4^+ level (µmol/L)
**
*
**
**
**
RPMI 8226 w Gln
RPMI 8226 w/o Gln
OPM2 w Gln
OPM2 w/o Gln
JJN3 w Gln
JJN3 w/o Gln
KMS-12-BM w Gln
KMS-12-BM w/o Gln
XG1 w Gln
XG1 w/o Gln
697 w Gln
697 w/o Gln
B
**P=.0027
**P=.0079
***P=.0002
****P<.0001
1000
800
600
400
200
0
NH_4^+ level (µmol/L)
HMCLs w Gln
HMCLs w/o Gln
MM CD138+ cells w Gln
MM CD138+ cells w/o Gln
MM CD138- cells w Gln
MM CD138- cells w/o Gln
C
*P=.042
250
200
150
100
50
0
NH_4^+ (µmol/L)
Indolent monoclonal gammopathies (MGUS and SMM)
MM
D
***P=.00064
800
600
400
200
0
Glutamine (µM)
MGUS and SMM
MM
E
***P=.00034
400
300
200
100
0
Glutamate (µM)
MGUS and SMM
MM

Figure 2

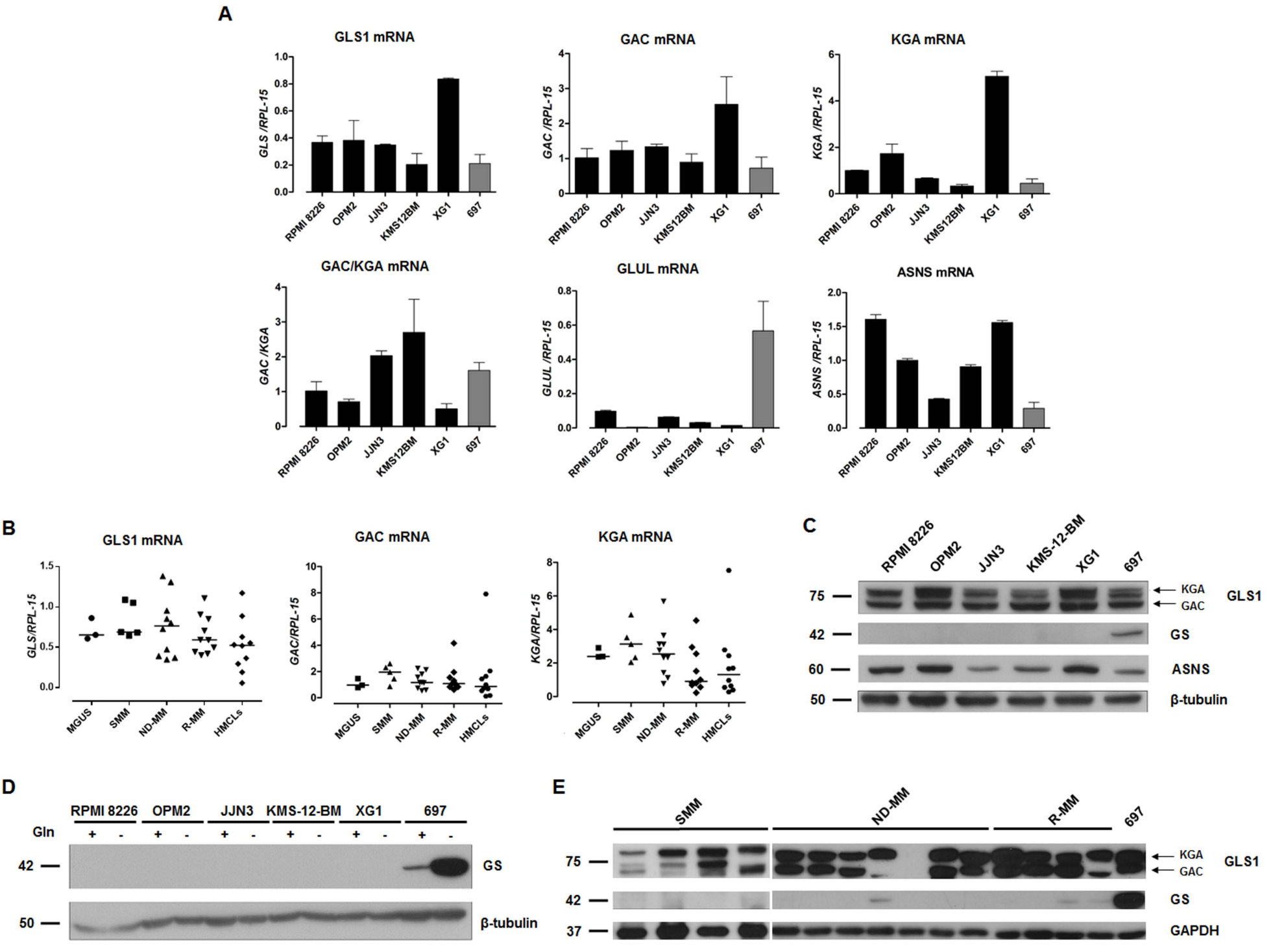
A
GLS1 mRNA
GLS /RPL-15
GAC mRNA
GAC /RPL-15
KGA mRNA
KGA /RPL-15
GAC/KGA mRNA
GAC /KGA
GLUL mRNA
GLUL /RPL-15
ASNS mRNA
ASNS /RPL-15
RPMI 8226
OPM2
JJN3
KMS12BM
XG1
697
B
GLS1 mRNA
GLS/RPL-15
GAC mRNA
GAC/RPL-15
KGA mRNA
KGA/RPL-15
MGUS
SMM
ND-MM
R-MM
HMCLs
C
RPMI 8226
OPM2
JJN3
KMS-12-BM
XG1
697
75
42
60
50
KGA
GAC
GLS1
GS
ASNS
β-tubulin
D
RPMI 8226
OPM2
JJN3
KMS-12-BM
XG1
697
Gln
+ - + - + - + - + - + -
42
50
GS
β-tubulin
E
SMM
ND-MM
R-MM
697
75
42
37
KGA
GAC
GLS1
GS
GAPDH

Figure 3

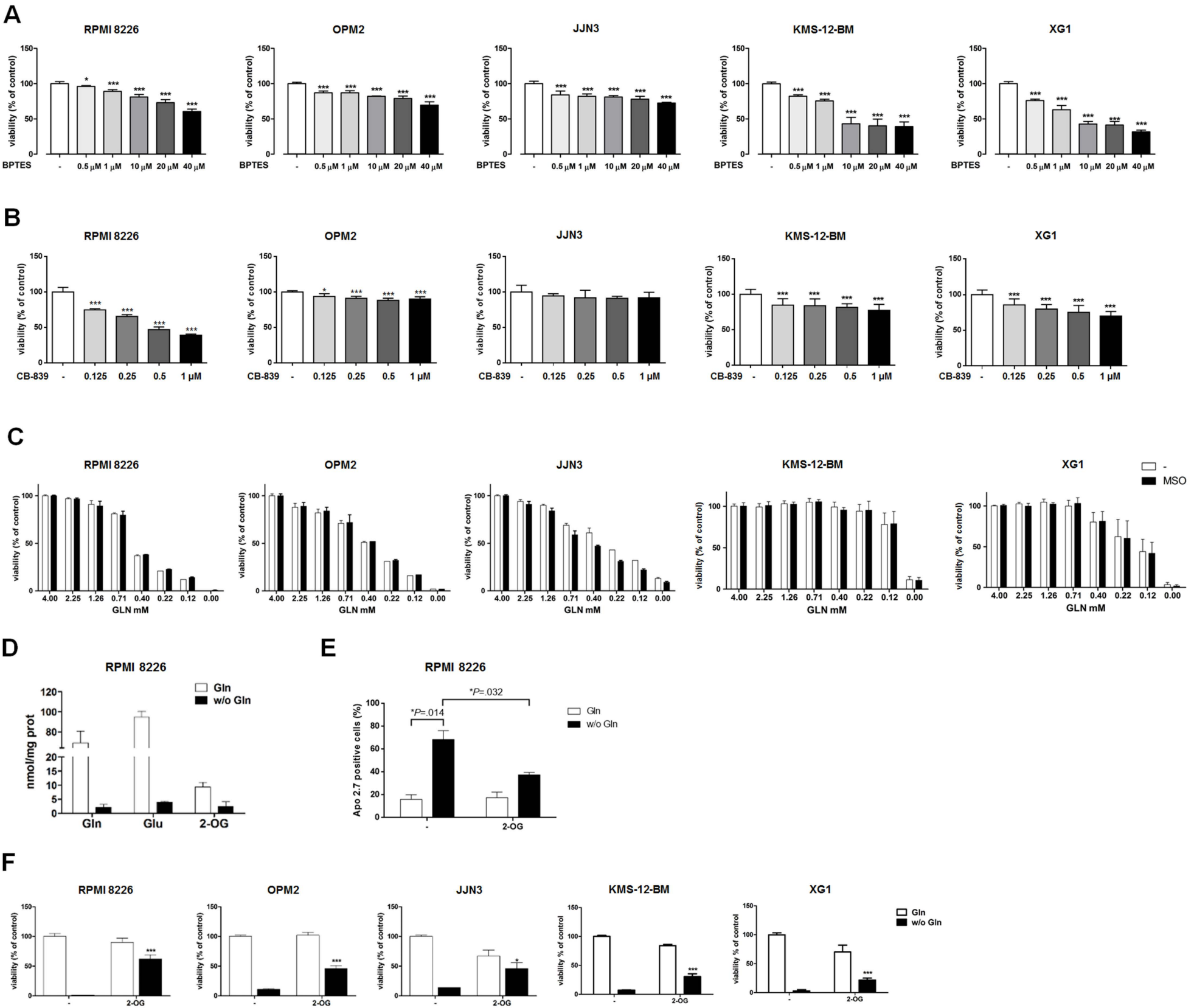
A
RPMI 8226
OPM2
JJN3
KMS-12-BM
XG1
viability (% of control)
BPTES
- 0.5 μM 1 μM 10 μM 20 μM 40 μM
B
CB-839
- 0.125 0.25 0.5 1 μM
C
GLN mM
4.00 2.25 1.26 0.71 0.40 0.22 0.12 0.00
-
MSO
D
nmol/mg prot
Gln
w/o Gln
Gln Glu 2-OG
E
Apo 2.7 positive cells (%)
*P=.014
*P=.032
2-OG
F

Figure 4

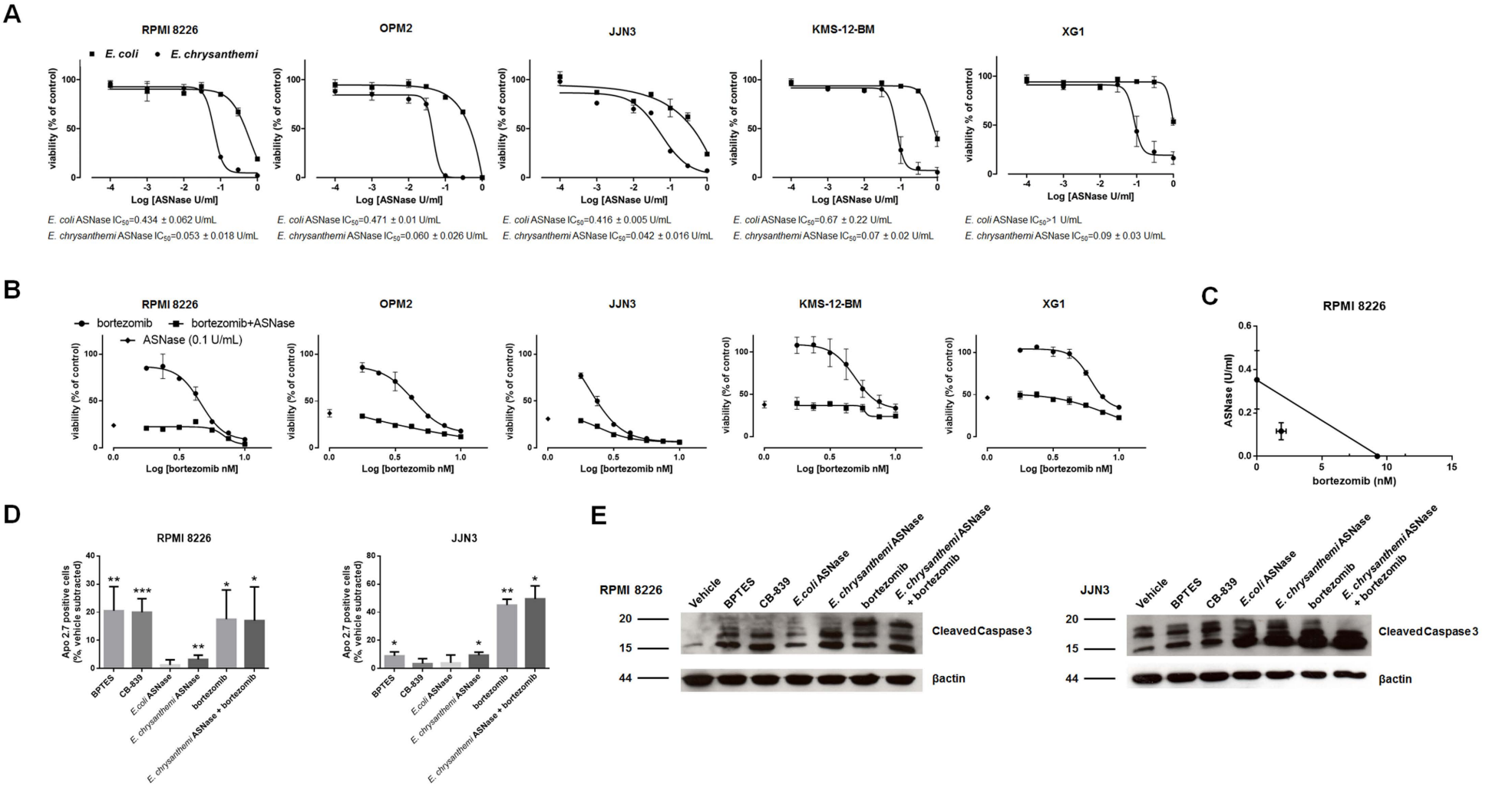
A
RPMI 8226
OPM2
JJN3
KMS-12-BM
XG1
E. coli
E. chrysanthemi
viability (% of control)
Log [ASNase U/ml]
E. coli ASNase IC50=0.434 ± 0.062 U/mL
E. chrysanthemi ASNase IC50=0.053 ± 0.018 U/mL
E. coli ASNase IC50=0.471 ± 0.01 U/mL
E. chrysanthemi ASNase IC50=0.060 ± 0.026 U/mL
E. coli ASNase IC50=0.416 ± 0.005 U/mL
E. chrysanthemi ASNase IC50=0.042 ± 0.016 U/mL
E. coli ASNase IC50=0.67 ± 0.22 U/mL
E. chrysanthemi ASNase IC50=0.07 ± 0.02 U/mL
E. coli ASNase IC50>1 U/mL
E. chrysanthemi ASNase IC50=0.09 ± 0.03 U/mL
B
RPMI 8226
OPM2
JJN3
KMS-12-BM
XG1
bortezomib
bortezomib+ASNase
ASNase (0.1 U/mL)
viability (% of control)
Log [bortezomib nM]
C
RPMI 8226
ASNase (U/ml)
bortezomib (nM)
D
RPMI 8226
JJN3
Apo 2.7 positive cells (% vehicle subtracted)
BPTES
CB-839
E.coli ASNase
E. chrysanthemi ASNase
bortezomib
E. chrysanthemi ASNase + bortezomib
E
RPMI 8226
JJN3
Vehicle
BPTES
CB-839
E.coli ASNase
E. chrysanthemi ASNase
bortezomib
E. chrysanthemi ASNase + bortezomib
Cleaved Caspase 3
βactin

Figure 5

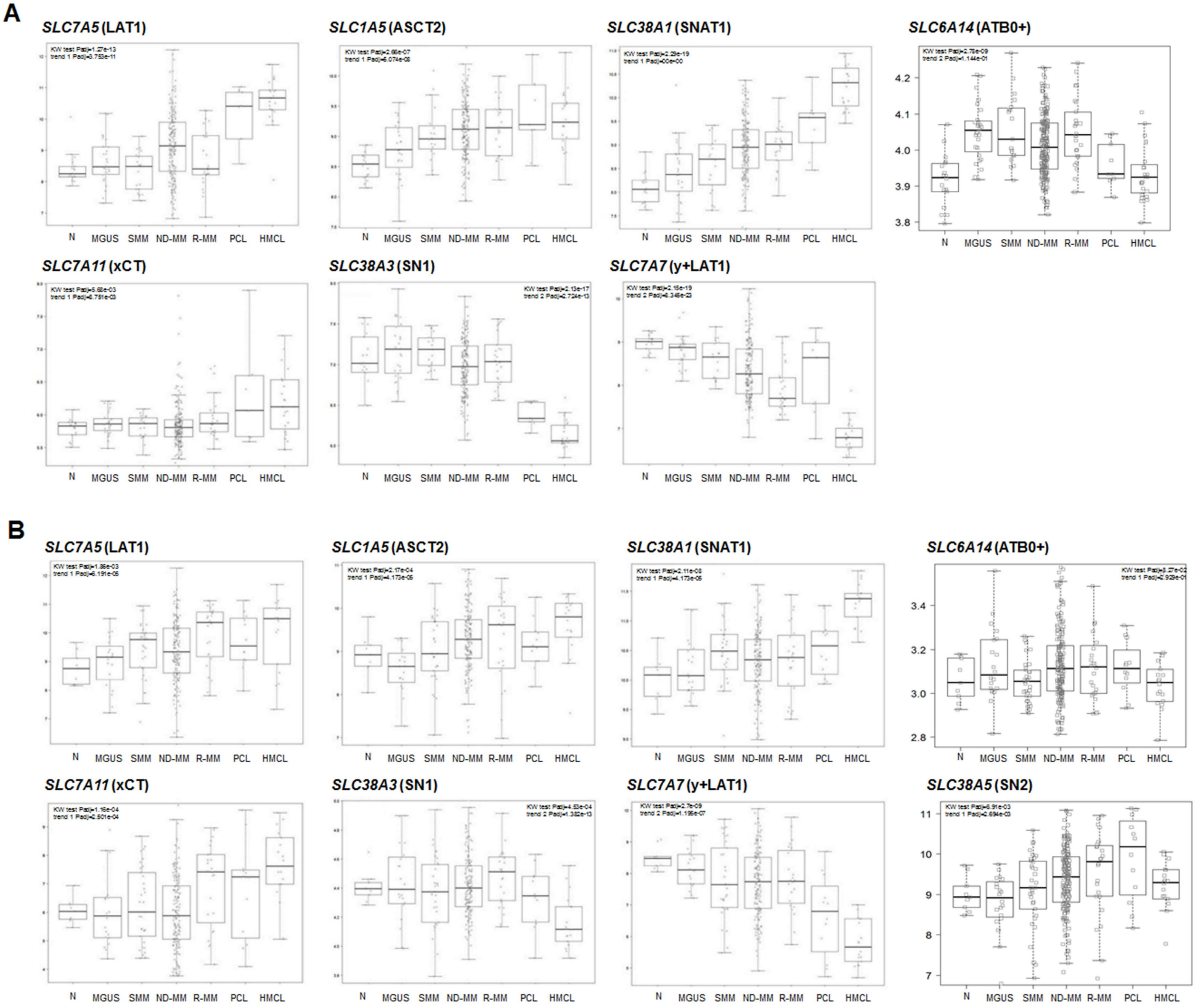
A
SLC7A5 (LAT1)
SLC1A5 (ASCT2)
SLC38A1 (SNAT1)
SLC6A14 (ATB0+)
SLC7A11 (xCT)
SLC38A3 (SN1)
SLC7A7 (y+LAT1)
B
SLC7A5 (LAT1)
SLC1A5 (ASCT2)
SLC38A1 (SNAT1)
SLC6A14 (ATB0+)
SLC7A11 (xCT)
SLC38A3 (SN1)
SLC7A7 (y+LAT1)
SLC38A5 (SN2)
N MGUS SMM ND-MM R-MM PCL HMCL

Figure 6

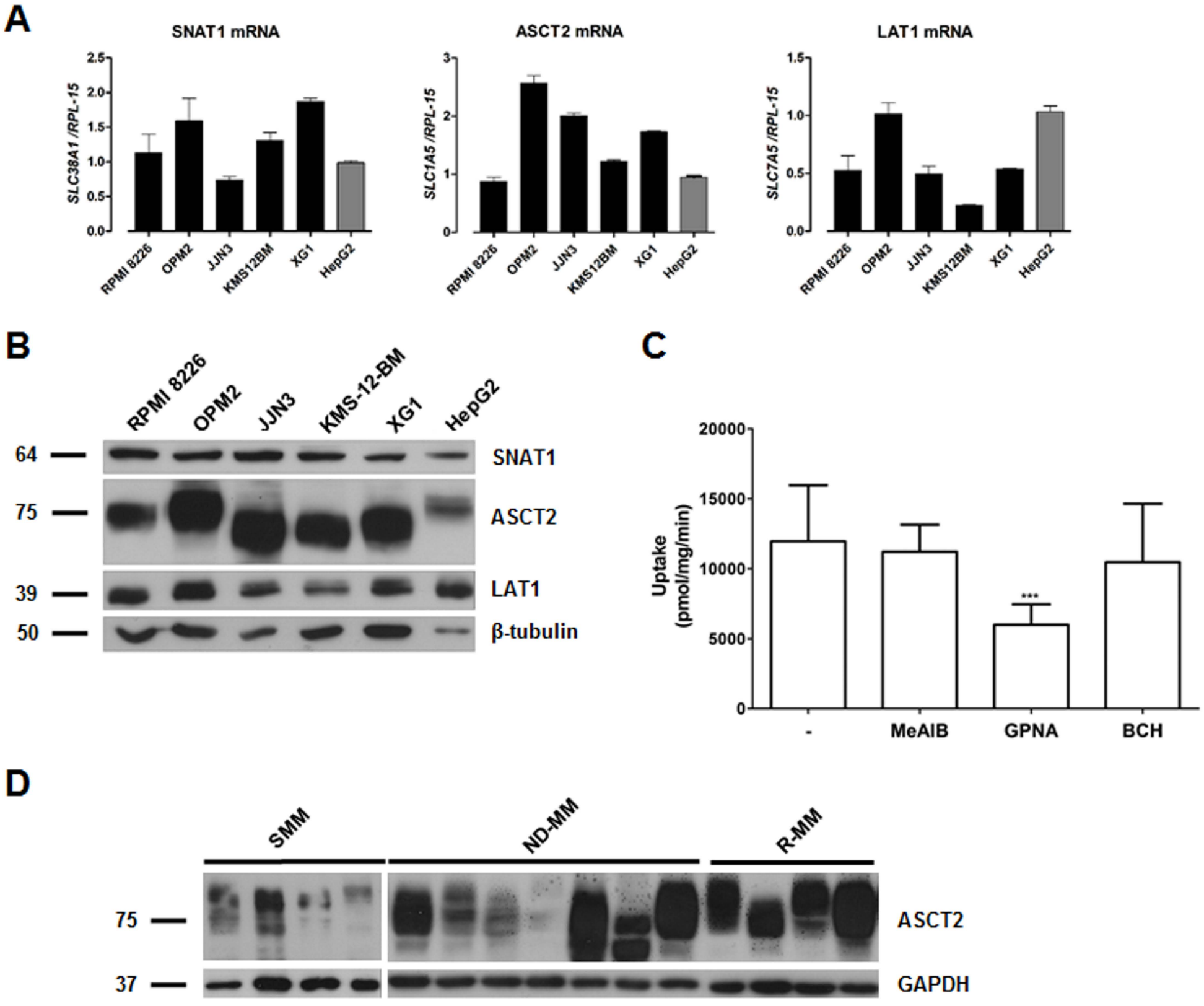
A
SNAT1 mRNA
SLC38A1 /RPL-15
ASCT2 mRNA
SLC1A5 /RPL-15
LAT1 mRNA
SLC7A5 /RPL-15
RPMI 8226
OPM2
JJN3
KMS12BM
XG1
HepG2
B
RPMI 8226
OPM2
JJN3
KMS-12-BM
XG1
HepG2
64
75
39
50
SNAT1
ASCT2
LAT1
β-tubulin
C
Uptake (pmol/mg/min)
20000
15000
10000
5000
0
***
-
MeAIB
GPNA
BCH
D
SMM
ND-MM
R-MM
75
37
ASCT2
GAPDH

Figure 7

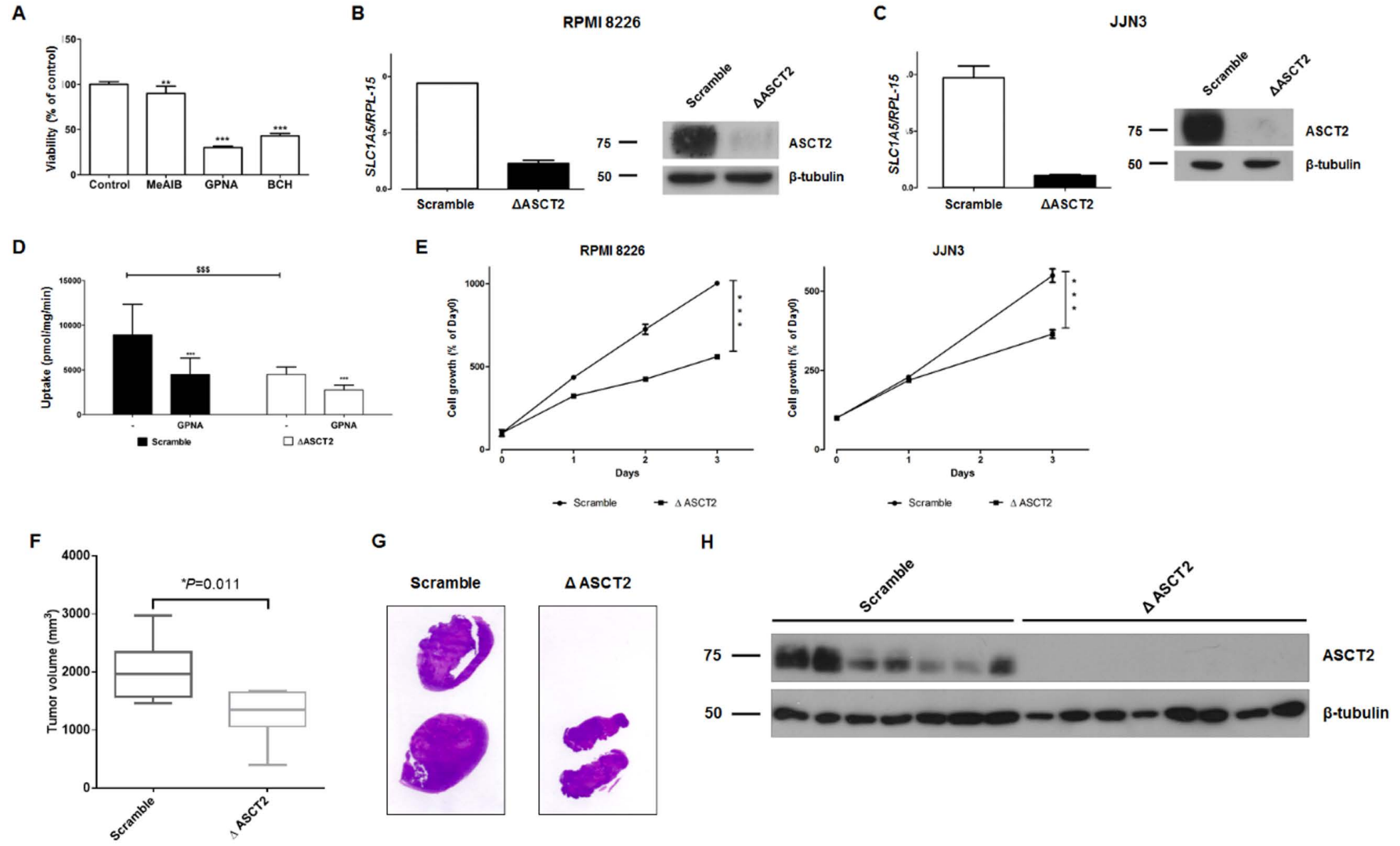
A
Viability (% of control)
Control
MeAIB
GPNA
BCH
B
RPMI 8226
SLC1A5/RPL-15
Scramble
ΔASCT2
75
50
ASCT2
β-tubulin
C
JJN3
D
Uptake (pmol/mg/min)
GPNA
Scramble
ΔASCT2
E
RPMI 8226
JJN3
Cell growth (% of Day0)
Days
Scramble
Δ ASCT2
F
*P=0.011
Tumor volume (mm³)
G
Scramble
Δ ASCT2
H
Scramble
Δ ASCT2
75
50
ASCT2
β-tubulin

From www.bloodjournal.org by guest on July 26, 2016. For personal use only.

Prepublished online June 6, 2016;
doi:10.1182/blood-2016-01-690743

Dependence on glutamine uptake and glutamine addiction characterize myeloma cells: a new attractive target

Marina Bolzoni, Martina Chiu, Fabrizio Accardi, Rosanna Vescovini, Irma Airoldi, Paola Storti, Katia Todoerti, Luca Agnelli, Gabriele Missale, Roberta Andreoli, Massimiliano G. Bianchi, Manfredi Allegri, Amelia Barilli, Francesco Nicolini, Albertina Cavalli, Federica Costa, Valentina Marchica, Denise Toscani, Cristina Mancini, Eugenia Martella, Valeria Dall'Asta, Gaetano Donofrio, Franco Aversa, Ovidio Bussolati and Nicola Giuliani

Information about reproducing this article in parts or in its entirety may be found online at:
http://www.bloodjournal.org/site/misc/rights.xhtml#repub_requests

Information about ordering reprints may be found online at:
http://www.bloodjournal.org/site/misc/rights.xhtml#reprints

Information about subscriptions and ASH membership may be found online at:
http://www.bloodjournal.org/site/subscriptions/index.xhtml

Advance online articles have been peer reviewed and accepted for publication but have not yet appeared in the paper journal (edited, typeset versions may be posted when available prior to final publication). Advance online articles are citable and establish publication priority; they are indexed by PubMed from initial publication. Citations to Advance online articles must include digital object identifier (DOIs) and date of initial publication.

Blood (print ISSN 0006-4971, online ISSN 1528-0020), is published weekly by the American Society of Hematology, 2021 L St, NW, Suite 900, Washington DC 20036.
Copyright 2011 by The American Society of Hematology; all rights reserved.